Journal of Electroanalytical Chemistry 840 (2019) 93–100

Contents lists available at ScienceDirect

Journal of Electroanalytical Chemistry

journal homepage: www.elsevier.com/locate/jelechem

Construction of an electrochemical genosensor based on screen-printed gold electrodes (SPGE) for detection of a mutation in the *adenomatous polyposis coli* gene

Luis Fernando Garcia-Melo[a,b], Isela Álvarez-González[a], Eduardo Madrigal-Bujaidar[a], Eduardo O. Madrigal-Santillán[c], José Antonio Morales-González[c], Rosa Natali Pineda Cruces[b], Jorge Alfredo Campoy Ramírez[b], Pablo Damian Matsumura[d], María de los Angeles Aguilar-Santamaría[e], Nikola Batina[b,*]

[a] Laboratorio de Genética, Escuela Nacional de Ciencias Biológicas, Instituto Politécnico Nacional, Avenida Wilfrido Massieu s/n, Col. Zacatenco, Del. Gustavo A. Madero, CP 07738 Ciudad de México, Mexico
[b] Laboratorio de Nanotecnología e Ingeniería Molecular, Área Electroquímica, Departamento de Química, CBI, Universidad Autónoma Metropolitana-Iztapalapa (UAM-I), Av. San Rafael Atlixco 186, Iztapalapa, CP 09340 México City, Mexico
[c] Laboratorio de Medicina de Conservación, Escuela Superior de Medicina, Instituto Politécnico Nacional, "Unidad Casco de Santo Tomás", Plan de San Luis y Díaz Mirón, Ciudad de México, CP 11340, Mexico
[d] Laboratorio de Endocrinología Molecular, Departamento de Biología de la Reproducción, CBS, Universidad Autónoma Metropolitana-Iztapalapa (UAM-I), México City, Mexico
[e] Laboratorio de Genética, Departamento de Ciencias de la Salud, CBS, Universidad Autónoma Metropolitana-Iztapalapa (UAM-I), México City, Mexico

ARTICLE INFO

Keywords:
Gene detection
Electrochemical genosensor
APC genosensor
Doxorubicin

ABSTRACT

Studies have well documented that mutations in the *adenomatous polyposis coli* gene (*APC*) are involved in the development of different types of cancer. Therefore, the objective of the present report was to design and construct a sensitive nanostructured genosensor able to detect specific sequences of the *APC* gene in order to be applied in early carcinogenesis diagnosis. We used screen-printed gold electrodes (SPGE) modified with DNA probes and mercaptoundecanoic acid chemically immobilized on a gold sensor surface. *APC* complementary DNA sequences were hybridized on the previously immobilized DNA probes. Besides, we tested effects of different intercalating agents, and various temperatures on the hybridization reaction to increase the sensitivity and selectivity of our device. The evaluation of these processes was carried out by means of the cyclic voltammetry technique (CV) to monitor the redox reaction of $[Fe(CN)_6]^{3-/4-}$ on the SPGE-s. The constructed genosensor exhibited an excellent response to identify the *APC* gene in a concentration range from 100 pM to 100 μM, with 43.92 pM as the limit of detection in the presence of doxorubicin as DNA intercalating agent. The selectivity of the device was tested by using a DNA sequence different from the *APC* gene, which shows negative response. Considering the importance of *APC* mutations in the development of tumors in the digestive, urogenital, and mammary tissues, here developed electrochemical genosensor, due to its easy management, short time of response, and high performance, may be useful for early cancer detection.

1. Introduction

The *adenomatous polyposis coli* gene (*APC*) is situated in the chromosome 5q21, and is known to act as tumor suppressor gene [1]. *APC* codify the protein APC, which in turn antagonizes the wingless-type signaling pathway by joining and regulating *β-catenin* in the intestine, skin, and immunologic system, as well as in bone and brain tissues [1,2]. Moreover, the mentioned protein is involved in various crucial

Abbreviations: APC, *Adenomatous polyposis coli*; SPGE, Screen-printed gold electrodes; CV, Cyclic voltammetry; MUC, 11-mercaptoundecanoic acid; ssDNA, Probe Sequence; dsDNA, *APC* complementary target; sNC, Non-complementary Sequence; MUCS, 11-mercaptoundecanoic acid + Probe Sequence solution; PBS, Phosphate buffered saline pH 7.4; DOX, Doxorubicin; PI, Propidium iodide; HC, Höechst 33258; AO, Acridine orange; EB, Ethidium bromide; MB, Methylene blue; IT, Intercalating agents

* Corresponding author.
E-mail address: bani@xanum.uam.mx (N. Batina).

https://doi.org/10.1016/j.jelechem.2019.03.048
Received 21 December 2018; Received in revised form 20 March 2019; Accepted 22 March 2019
Available online 27 March 2019
1572-6657/

cellular and biochemical processes including migration, adhesion, differentiation, proliferation, apoptosis, transcription and DNA repair [1,3]. Understandably then, a mutation in the indicated gene may give rise to abnormal codons that usually have tumorigenic properties [4]. A number of studies have shown that alterations in such gene are closely related with the development of tumors in various organs, including prostate, liver, pancreas, esophagus, and breast [3,5–9], as well as in the stomach, colon and rectum [5].

The involvement of the *APC* gene in the carcinogenic process, and particularly the fact that its activity has been detected since the early progression phase of carcinogenesis [9–11], clearly suggest that abnormal expressions of such gene can be utilized as an early diagnostic biomarker. In this aspect, the development of tools for the early diagnosis of cancer is mandatory to avoid or reduce the diagnosis in advanced stages of the disease, and to improve the patient's prognosis, including a better quality and extent of life. Moreover, considering the complex genetic and epigenetic changes involved in the development of cancer, early diagnostic procedures should be very useful to high-risk individuals before the application of conventional cancer detection methods [12,13].

In this context, the construction of DNA electrochemical sensors is of a special importance due to their high sensitivity, specificity and capacity to analyze a large number of samples in a short time and no matter their relatively facile use and low cost [14]. Such devices are based on the immobilization of a single oligonucleotide chain probe on the surface of an electrochemical transductor, and on their ability to recognize the complementary DNA sequence (sample) through the hybridization process [15,16]. Commonly, the hybridization reaction on the electrode surface is confirmed by the changes observed in the hybridized DNA [17]. To increase the signal detection capacity of electrochemical sensors, researchers have proposed the use of electroactive molecules with the capacity to be intercalated in the DNA, including metallic cationic complexes, or organic compounds; these last ones have usually given rise to a more specific hybridization-signal relationship [18,19]. The critical aspect in the design and construction of genosensors is the finding of compounds with the capacity to form stable, compact and nano-ordered monolayers, thereby making it possible to avoid the background electric current, to inhibit corrosion, and to resist the ion penetration; so these compounds can act as effective barriers against electron transference [20,21]. The use of thiols has given good results to achieve such purposes because these molecules, besides complying with the previously mentioned characteristics, also propitiate a vertical conformation of the DNA molecule on the electrode surface, thus favoring the oligonucleotide hybridization [22]. Two other important factors that must be considered in the construction of a genosensor are the length of the thiol molecule, and the chemical nature of the functional terminal group; these aspects are necessary for the control of the monolayer properties, including the access to the genosensor active sites [23]. Besides, genosensors are superior to the traditional devices because they have shown higher design flexibility, excellent reproducibility and elevated hybridization efficacy [23,24]. Based on the above mentioned antecedents, the aim of the present research was to design and construct a high sensitivity genosensor with the capacity to detect specific sequences of the *APC* gene. For such a purpose we employed screen-printed gold electrodes (SPGE), and the electrochemical method, cyclic voltammetry (CV). Such device, which has not been previously reported for detection of the early and opportune identification of mutations in the *APC* gene, can also be used for the study of other cancer related DNA mutations.

2. Material and methods

2.1. Reagents

Potassium ferricyanide ($[Fe(CN)_6]^{3-}$), Potassium ferrocyanide ($[Fe(CN)_6]^{4-}$), phosphate buffered saline pH 7.4 (PBS), 11-mercaptoundecanoic acid (MUC), ethylenediaminetetraacetic acid (EDTA), Trizma® hydrochloride (Tris-Cl), doxorubicin (DOX), propidium iodide (PI), Höechst 33258 (HC), acridine orange (AO), ethidium bromide (EB), and methylene blue (MB) were purchased from Sigma Chemicals (St Louis, MO). Potassium ferrocyanide was obtained from Merck (Mexico), and ultrapure sodium dodecyl sulfate (SDS) was purchased from MP Biomedicals, Inc. (Solon, OH). All solutions were prepared with ultrapure water from a Millipore Milli-Q system (resistivity 18.2 MΩcm) Millipore Corporation (Milford, MA).

The DNA oligonucleotides were purchased from T4oligo Company (Irapuato, Gto). Stock solutions of oligonucleotides were prepared with TE buffer (formed by 10 mM Tris-HCl, and 1 mM EDTA, pH 8.0) and stored in a freezer at −20 °C until use. Diluted solutions made in PBS 0.01 M at pH 7.4 in a range of 10^{-10} M to 10^{-4} M were prepared. The oligonucleotide sequences used in the experiments were the following:

Probe Sequence (ssDNA): 5′-SH-$(CH_3)_6$-GGT GGA GAT CTG CAA ACC TC-3′

APC complementary target (dsDNA): 5′-GAG GTT TGC AGA TCT CCA CC-3′

Non-complementary Sequence (sNC): 5′-GGT GGA GAT CTG CAA ACC TC-3′.

2.2. Apparatus

We used screen-printed gold electrodes (SPGE) (DRP 250AT from DropSens, Oviedo, Spain), as working electrode, Pt as counter electrode, and Ag/AgCl as reference electrode. CV was carried out at room temperature with a Bionalytical Systems BAS-100 electrochemistry workstation (West Lafayette, IN, USA). All potentials were referred to Ag/AgCl reference electrode. A new SPGE was used for each assay.

2.3. Preparation of the genosensor

In order to modify the working Au electrode, only the gold surface was incubated for 30 min, in 40 μL of 100 μM thiolated probe sequence (ssDNA) and MUC 1 μM (3:1) diluted in PBS 0.01 M. After this step, the SPGE was rinsed with 0.1% SDS diluted in PBS, and then with Milli-Q water to remove the non-adsorbed residuals. In this way the working gold electrodes become permanently modified with MUCS adlayer (MUC + ssDNA = MUCS).

2.4. Hybridization assay

In a further process, the Au surface modified with MUCS was incubated in 40 μL of 100 μM target DNA sequence. The hybridization reaction with oligonucleotides was carried out for 30 min at room temperature. Then, electrodes were rinsed with 0.1% SDS diluted in PBS, as well as with Milli-Q water in order to remove the unbound targets.

2.5. Sensitivity of the genosensor

The SPGE with the previously modified MUCS/Au electrode surface was incubated in 40 μL of target DNA sequence in concentrations of 100 pM, 1 nM, 10 nM, 100 Nm, 1 μM, 10 μM and 100 μM. The hybridization reaction with the oligonucleotides was carried out for 30 min at room temperature. Then, the electrodes were rinsed with 0.1% SDS diluted in PBS, and then with Milli-Q water.

2.6. Hybridization indicators

The dsDNA/MUCS/Au modified electrode surfaces were incubated with the following hybridization indicators (intercalating agents, IT): DOX, EB, PI, AO, HC, and MB. For this purpose, samples were treated with 10 μL of 20 μM IT/ 0.01 M PBS solution, for 20 min at room temperature in the dark. Note, in all electrochemical experiments,

concentration of the supporting electrolyte was 0.01 M PBS. After the incubation, electrodes were rinsed three times first with Milli-Q water and then with 0.01 M PBS.

2.7. Hybridization temperature

In order to maximize the sensitivity of our device we investigated the influence of temperature on the hybridization by examining its effect at 20, 37, 40, 45, 50 and 55 °C for 30 min, in 40 μL containing 1 μM of target DNA sequence solution, using the US autoflow automatic CO_2 (NU-4750) incubator (NuAire, Plymouth, MN). In addition, we evaluated the effect of DOX after the hybridization reaction; in this case, we used 10 μL of the compound (20 μM, diluted in PBS) for 20 min in the dark, at room temperature.

2.8. Selectivity of the genosensor

The detection capacity of the developed biosensor previously modified (MUCS/Au) was tested. The genosensor was incubated for 30 min at room temperature with 40 μL of 1 μM non-complementary sequence (sNC). Then, the electrode was rinsed with 0.1% SDS diluted in PBS, and with Milli-Q water. Later, the genosensor was incubated with 40 μL containing 1 μM of target DNA sequence for 30 min at room temperature. Finally, the electrode was rinsed with 0.1% SDS diluted in 0.01 M PBS, and with Milli-Q water.

One electrode modified with sNC/MUCS/Au, and another modified with dsDNA/MUCS/Au were incubated in the dark with 10 μL containing 20 μM of DOX in 0.01 M PBS solution, for 20 min at room temperature. After the incubation, electrodes were rinsed three times first with Milli-Q water and then with 0.01 M PBS.

2.9. Electrochemical measuring

The electrochemical detection was made by means of CV at a scan rate of 50 mV/s, within a potential range from −400 mV to +500 mV and we used the second scan in positive sense. The CV measurements were carried out with a drop of 150 μL of 2.5 mM $[Fe(CN)_6]^{3-/4-}$ diluted in 0.01 M PBS (pH 7.4). Such mix corresponds to the redox probe placed on the electrode surface at room temperature.

3. Results and discussion

Fig. 1A shows the redox peaks obtained for the $[Fe(CN)_6]^{3-/4-}$ probe, using unmodified and modified SPGE in the CV mode. The general redox equation for all process is the next: $[Fe(III)(CN)_6]^{3-} + e^- \leftrightarrow [Fe(II)(CN)_6]^{4-}$. The maximum current of $[Fe(CN)_6]^{3-/4-}$ of the anodic peak (i_{pa}) was measured to 73.42 ± 0.87 μA for unmodified SPGE, line (a), at 164 mV. A pertinent statement here is that PBS solution did not show any electrochemical signal that could affect the $[Fe(CN)_6]^{3-/4-}$ redox reaction (as it is show text later). Line (b) represents the cyclic voltammogram obtained for the same system at the modified MUCS/Au electrode. In this case we observed a notable decrease in the $[Fe(CN)_6]^{3-/4-}$ current peak (anodic part): from 73.42 ± 1.23 to 68.1 ± 1.74 μA. The decrease of the first value (68.1 μA) corresponded to the maximum height of the MUCS/Au anodic peak, and in the process of the further assays, it represents 0% of DNA hybridization reaction with the target DNA *APC* gene. Therefore, any decrease of this anodic peak value would represent a progress of a hybridization reaction, as well as an increase in the transfer resistance of interfacial $[Fe(CN)_6]^{3-/4-}$ ions. This decrease can be related to the non-conducting capacity of the electrode surface modified by oligonucleotides [25]. Furthermore, the MUC barrier also avoids the access of the redox probe ions to the Au electrode, and consequently the current decrease [26]. Later and in addition, the device was subjected to hibridization reactions with 10^{-6} M and 10^{-4} M of the target DNA (lines (c) and (d), respectively). In this reaction, with respect to the value of MUCS/Au, we found a significant current reduction of 25.52% and of 78.81% to 10^{-6} M and 10^{-4} M of dsDNA/MUCS/Au. Such results confirm that the hydridization process was carried out. The observed decreases could be explained as a consequence of the blocking of the electrode active surface, as well as because of the steric hindrance after the hybridization. Another possibility to explain the results could be an increase in the negative charge, which can give rise to repellency of redox species on the electrode surface [27]. In this respect, Torati et al. [28] demonstrated that the differences in the peak current before and after the DNA interactions are related to the hybridization efficiency.

The analytical performance of the genosensor was evaluated using different concentrations of target DNA (from 100 pM to 100 μM, which means 10^{-10} M to 10^{-4} M). Fig. 1B represents the maximum current of $[Fe(CN)_6]^{3-/4-}$ of the anodic peak obtained of the cyclic voltammogram for each concentration of the dsDNA/MUCS/Au used in the hybridization process. In the figure, we show that the maximum anodic peak for MUCS/Au was found at 69.63 μA, a value that decreased to 26.25 μA due to an increase in the target DNA concentration in dsDNA/MUCS/Au electrode. Simply, this means that increases in the presence of genetic material in the sample led to the decrease of the anodic peak current of the $[Fe(CN)_6]^{3-/4-}$ probe. According to Avelino et al. [29], electrochemical $[Fe(CN)_6]^{3-/4-}$ signal is decreased/suppressed due to blocked electron flux through the electrode surface covered by genetic material.

To determine the detection capacity of the genosensor, we calculated the relative percentage of the anodic peak diminution vs. target DNA concentration, in the range from 100 pM to 100 μM. For each of the used concentrations, the capacity of hybridization was calculated with the following equation: $\%\ I_{Relative} = [(I_0 - I_m)/I_0] * 100$, where I_0 is the maximum anodic peak of MUCS/Au and I_m corresponds to the maximum anodic peak of the dsDNA/MUCS/Au current after the hybridization reaction. Fig. 1C shows the linear correlation between the logarithms of the target DNA concentration with $I_{Relative}$ (%), whose linear regression coefficient was $R^2 = 0.95496$. A gradual percentage decrease was observed with respect to the concentration increase of the target DNA. The detection limit based on the dsDNA/MUCS/Au for determined according to the $3 \times S_b$ criterion, where S_b was estimated as the standard deviation of the blank measurements and fitting to the respective equation of the linear portion of the plot. A detection limit f 3.604×10^{-10} M was estimated and the regression equation was as follows: $\%\ I_{Relative}$ (μA) = 59.089 + 6.175 log target DNA concentration (M). The limit of detection was estimated according to Li et al. [30]. Based on these results, we decided to use 1 μM of target DNA in subsequent assays dedicated to improve the sensitivity of the device.

In view of the fact that IT-s have been reported to increase the hybridization efficiency [31–34], we tested the effect of these chemicals to improve the sensitivity of our genosensor. Therefore, we compared the electrochemical response of the 2.5×10^{-6} M $[Fe(CN)_6]^{3-/4-}$ probe on the dsDNA/MUCS/Au electrode in the presence of DOX, OA PI, EB, HC and MB. Fig. 2 shows the effect induced by the intercalating chemicals. Red bar shows the electrochemical response in $\%\ I_{relative}$ values when different IT-s, were used. For each of the IT-s, the capacity of increase the hybridization efficiency was calculated with the following equation: $\%\ I_{Relative} = [(I_0 - I_m)/I_0] * 100$, where I_0 is the maximum anodic peak of dsDNA/MUCS/Au and I_m corresponds to the maximum anodic peak of the IT/dsDNA/MUCS/Au current after the hybridization reaction. The concentration of the IT-s was kept constant: 2×10^{-6} M. Note, no faradic peaks in the investigated potential range were observed, to be assigned specifically for IT species. However, all tested IT-s induce a decreased of the dsDNA/MUCA/Au anodic peak, which clearly shows the expected effect of the intercalation agents on the DNA hybridization reaction. According to the literature, such effect can be related to induction of negative charges in the electrode layer and therefore repulsion with the negatively charged $[Fe(CN)_6]^{3-/4-}$ ions [35–37]. In the same way, the different reaction conditions could

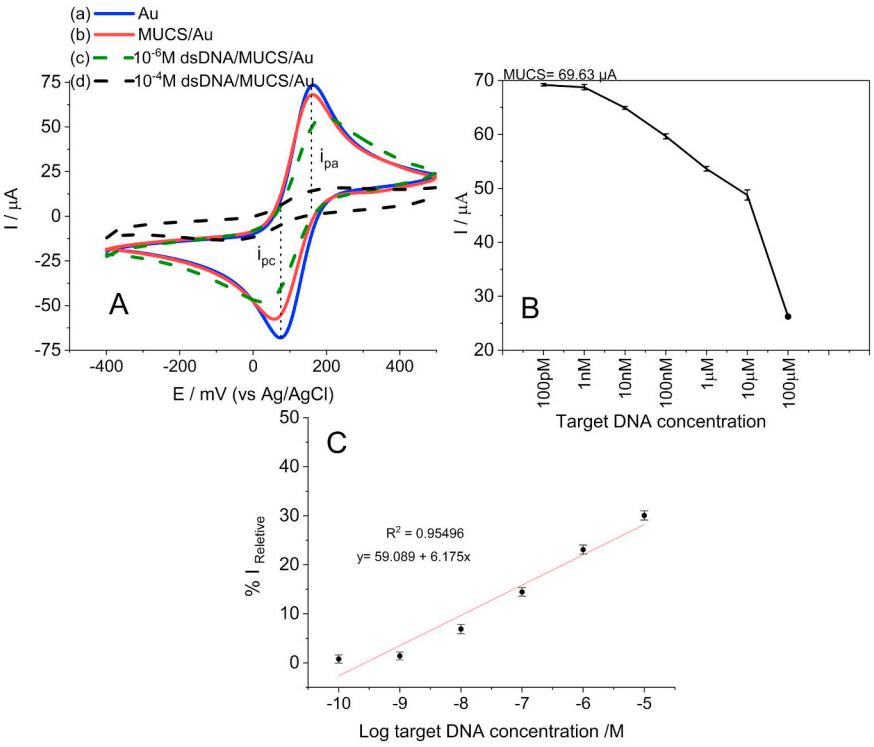

Fig. 1. (A) Cyclic voltammograms current of the 20 mM $[Fe(CN)_6]^{3-/4-}$ redox probe/0.01 M PBS (pH 7.4), registered on unmodified Au electrode (a), modified MUCS/Au electrode (b), 10^{-6} M dsDNA/MUCS/Au electrode (c), and 10^{-4} M dsDNA/MUCS/Au electrode (d).
(B) Plot of CV anodic peak current vs target DNA concentration.
(C) Linear relationship between the relative current change (% $I_{Relative} = [(I_0 - I_m)/I_0] * 100$) of the anodic peak of the $[Fe(CN)_6]^{3-/4-}$ redox probe and the logarithm of the target DNA concentration.
All electrochemical measures was made by means of cyclic voltammetry (CV) at a scan rate of 50 mV/s, within a potential range from −400 mV to +500 mV.

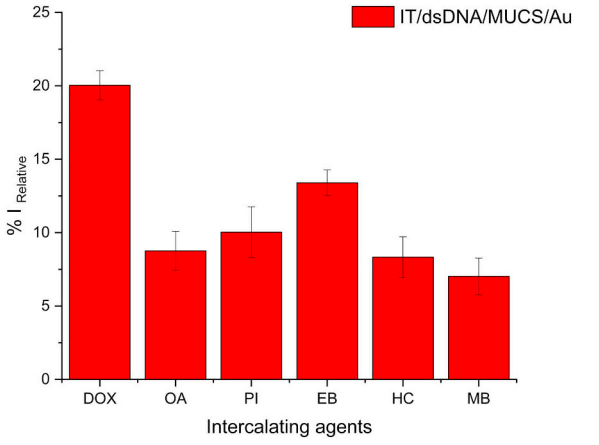

Fig. 2. Effect of the intercalating agents (IT-s) on the DNA hybridization reaction.
Relative current change (% $I_{Relative} = [(I_0 - I_m)/I_0] * 100$) of the anodic peak of modified IT/dsDNA/MUCS/Au (red bars) in relation to dsDNA/MUCS/Au. It shows effect of intercalating agents: doxorubicin (DOX), propidium iodide (PI), Höechst 33,258 (HC), acridine orange (AO), ethidium bromide (EB), and methylene blue (MB) on the DNA hybridization reaction.

affect the results [38]. It has been observed that intercalating agents inserted between the base pairs of DNA, which results in a decrease in the helical turn of the DNA and promotes its elongation, directly affecting the sugar-phosphate skeleton bonds forming a large groove in the most cases [39–41]. Therefore, the DNA molecule could build more compact layers. As well, the aromatic hydrophobic regions of the IT are attracted to similar zones of nitrogenous DNA bases, increasing diffusion of IT molecules [42,43]. Another phenomenon, which has been observed is that IT is capable to reduce the effective charge density of DNA [31,41,44,45]. In addition, it is known that IT molecules could interact with the genetic material at different ways: forming T-shaped, not stacked and face-to-face complexes [46,47]. According to literature, the IT stabilize the DNA chains due to the improvement of the base stacking process, the increase in the hydrogen bridge interaction and the van der Waals forces, as well as the electrostatic interactions. In this way IT could improve the spatial conformation of the DNA, and avoid the flux of $[Fe(CN)_6]^{3-/4-}$ ions to the electrode surface [48,49]. Although we do not know the exact mechanism of the used IT-s, we could clearly see that in the presence of the IT molecules hybridization reaction of DNA influence the structure of the modified electrode molecular layer and its permeability to $[Fe(CN)_6]^{3-/4-}$ ions. These actions, consequently, increase the sensitivity of the present genosensor to detection *APC* gene. We found that DOX had the stronger capacity to indicate the hybridization process; the results indicate an increase of 20.03 ± 1.03 for % $I_{Relative}$. Our results also show that DOX had the best capacity to interact with double chain DNA. Such effect can be explained considering that two of the three DOX rings were intercalated between guanine and adenine, while the ring of sugar remained outside of the duplex, interacting with the minor groove [48–50] [2–4]. Therefore, a complex was formed where the electrostatic charge of DOX was in the phosphate groups [48–51]. This interaction was favored by the formation of H bonds between the amino sugar and the site of the oxygen base [49,50]. Diminution of the anodic peak current observed in our experiments indicates that DOX was efficient IT agent and mostly preconcentrated between the dsDNA chains. DOX molecules do not show any electrochemical reaction at the SPGE surface as (it is show text later) [51].

Based on the results obtained with DOX, in the new step we evaluated the influence of the DOX presence on the dsDNA hybridization. Fig. 3A shows cyclic voltammetry curves of different unmodified and modified Au-electrodes obtained in 0.01 M PBS (pH 7.4). First, we characterized the unmodified gold surface, line (a). Line (b) shows electrochemical response of PBS buffer on the surface modification with DOX/dsDNA/MUCS/Au. Line (c) represents the effect of PBS buffer containing 2.5 µM DOX solutions on the surface of DOX/dsDNA/MUCS/Au. Finally, line (d) shows the electrochemical response obtained of PBS buffer containing 2.5 µM $[Fe(CN)_6]^{3-/4-}$. It is observed that PBS and DOX, do not affect the electrochemical response of the $[Fe(CN)_6]^{3-/4-}$ at the SPGE electrode. Similar responses of DOX were obtained in Yau et al. [51].

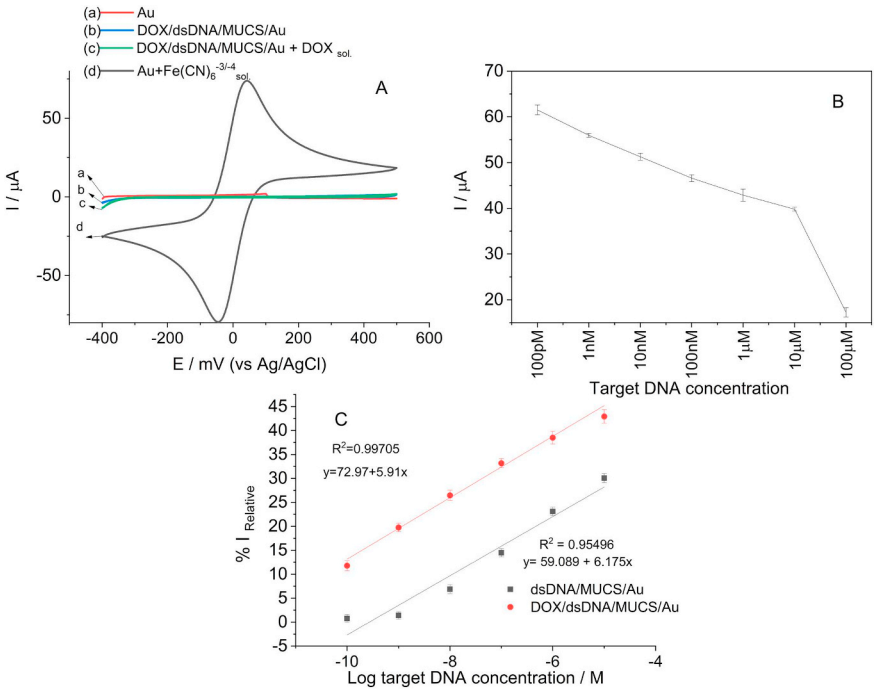

Fig. 3. Effect of DOX on the DNA hybridization reaction. (A) Cyclic voltammograms obtained for (a) unmodified Au electrode, (b) DOX/dsDNA/MUCS/Au, (c) DOX/dsDNA/MUCS/Au (in excess 10^{-5} M of DOX in solution), (d) corresponding cyclic voltammograms for unmodified Au electrode in 10^{-5} M $[Fe(CN)_6]^{3-/4-}$. All in 0.01 M PBS electrolyte solution.
(B) Anodic peak current for $[Fe(CN)_6]^{3-/4-}$ redox probe recorded at DOX/dsDNA/MUCS/Au electrode, in different concentration of target DNA.
(C) Linear relationship between the relative current change of the anodic peak $[Fe(CN)_6]^{3-/4-}$ redox probe and the logarithm of the target DNA concentration at DOX/dsDNA/MUCS/Au and dsDNA/MUCS/Au electrodes, respectively.
All electrochemical measures was made by means of cyclic voltammetry (CV) at a scan rate of 50 mV/s, within a potential range from −400 mV to +500 mV.

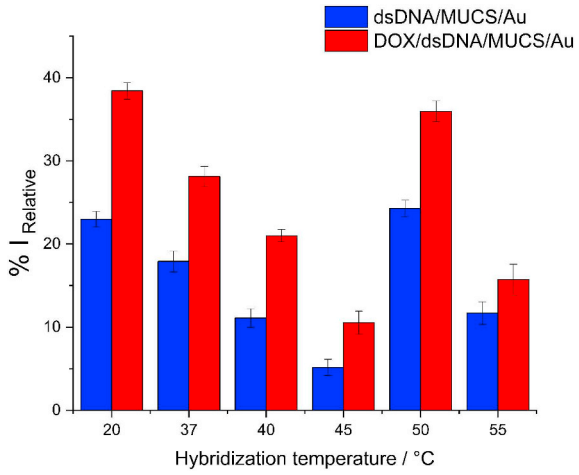

Fig. 4. Effect of temperature on the DNA hybridization reaction.
The relative current change of the anodic peak of $[Fe(CN)_6]^{3-/4-}$ redox probe vs hybridization temperature during to dsDNA/MUCS/Au preparation, before (blue) and after (red) the DOX treatment, at the room temperature (20 °C) (DOX/dsDNA/MUCS/Au).

In the next step, we evaluated the analytical behavior of the DNA biosensor using various concentrations of the target DNA to carry out the hybridization reaction on the gold surface (dsDNA/MUCS/Au). After the hybridization process, we added DOX at 20 µM (diluted in PBS) for 20 min at room temperature in the dark on the gold surface previously modified with dsDNA/MUCS/Au. Fig. 3B shows a gradual decrease of the anodic peak current $[Fe(CN)_6]^{3-/4-}$ redox probe at the electrode surface with addition of DOX with respect to the concentration increase in target DNA. In the range of 100 pM to 100 µM the current decreased from 69.19 µA to 26.248 µA. This result establishes that the use of DOX improved the sensitivity of our genosensor (Fig. 3C). The data present a linear correlation between the logarithm of the DOX/dsDNA/MUCS/Au concentration with $I_{Relative}$ (%), whose linear regression coefficient was 0.99705. The lowest limit of detection corresponded to 4.39×10^{-11} M (S/N = 3), and the regression equation was as follows: % $I_{Relative}$ (µA) = 72.97 + 5.91 log target DNA concentration (M). In addition, a comparison of two graphs for DOX/dsDNA/MUCS/Au and dsDNA/MUCS/Au, shows better sensitivity for sensor using DOX (Fig. 3).

Fig. 4, shows the effect of the hybridization temperature on the electrochemical response of the genosensor. Blue bars show a response after the hybridization reaction at dsDNA/MUCS/Au at different temperatures that range from 20 °C to 55 °C, without the presence of IT. The maximum blocking of the anodic peak current, expressed as % $I_{Relative}$ was obtained at 50 °C (24.28%). This result indicated the highest hybridization efficiency in the tested range of temperatures. It can be explained by an accumulation of negative charges in the electrode layer, such result generated by both: the formation of the fully hybridized probe-target duplexes, and the inhibition of the electron transfer at the electrode surface [52,53]. Wu et al. [54] have reported similar results. Furthermore, we demonstrated that value of % $I_{Relative}$ at 20 °C is 22.98%. Thus, we could conclude that hybridization reaction was also highly effective at 50 °C, as well as at 20 °C. The red bars represent the maximum anodic peak (% $I_{Relative}$) for same systems modified by DOX (DOX/dsDNA/MUCS/Au), after the hybridization process at different temperatures. It is important to mention that 20 µM DOX (diluted in PBS solution) was added for 20 min at room temperature in the dark, at the previously hybridized dsDNA/MUCS/Au electrodes. In such case, the best results with maximum effect for DOX/dsDNA/MUCS/Au electrode were achieved at 20 °C. Due to DOX treatment, the % $I_{Relative}$ increased additional for 15.43% in relation to dsDNA/MUCS/Au. In contrast, dsDNA/MUCS/Au formed at 50 °C, after treatment with DOX show an increase of the % $I_{Relative}$ for only 11.67%.

At general, it could be concluded that using DOX, the best effect on the sensor effectiveness is observed at experiments performed at 20 °C. In this context, Box [55] and Chu et al. [56] mentioned that the DNA interspacing capacity of DOX is related with the interaction of quinone, hydroxyquinone and the sugar group. These groups stabilize the DNA structure due to the hydrophobic stacking interactions between the DOX molecule and the adjacent base pairs, enhancing the delocalization of electron clouds. In addition, the stearic hindrance has been observed to increase by the immobilized compounds on the electrode surface [57–59] and consequently when the ion transfer is blocked on the electrode surface, the current decreases [60]. Besides, Vacek et al. [61] observed that the current decrease is due to the capacity of DOX to

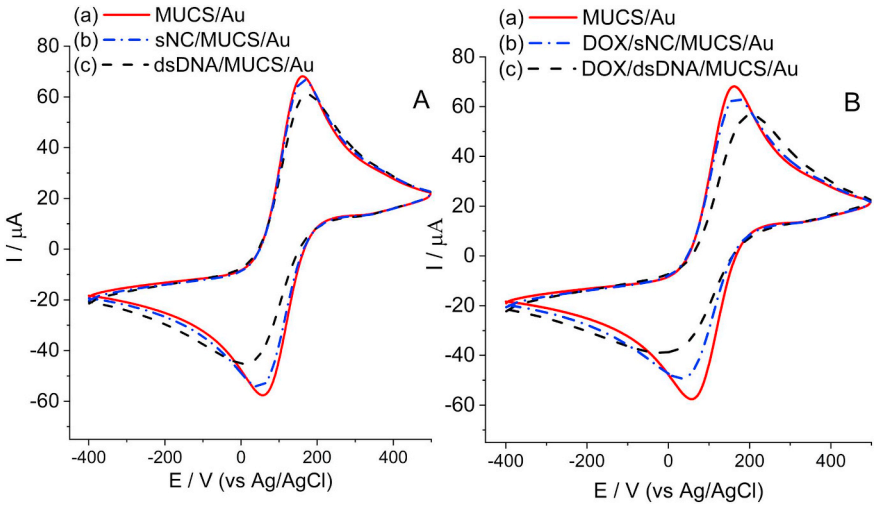

Fig. 5. The selectivity test of the genosensor. (A) Cyclic voltammograms of $[Fe(CN)_6]^{3-/4-}$ redox probe recorded at MUCS/Au electrode (a), sNC/MUCS/Au electrode (b), and dsDNA/MUCS/Au electrode (c). (B) Cyclic voltammograms of $[Fe(CN)_6]^{3-/4-}$ redox probe recorded at MUCS/Au electrode (a) DOX/sNC/MUCS/Au electrode (b), and DOX/dsDNA/MUCS/Au electrode (c). The DOX solution was added in excess 10^{-5} M. All electrochemical measures was made by means of cyclic voltammetry (CV) at a scan rate of 50 mV/s, within a potential range from −400 mV to +500 mV.

block the redox centers, as well as to the saturation of the DNA probes with complementary chains [35]. In summary, the main advantage of using DOX was to simplify the detection process and to increase the sensitivity of the device operating at room temperature.

Fig. 5A, shows cyclic voltammograms curves of SPGE modified with MUCS/Au, sNC/MUCS/Au, and dsDNA/MUCS/Au. Line (a) indicates that the maximum anodic peak of $[Fe(CN)_6]^{3-/4-}$ after the modification with MUCS/Au is 68.14 µA at a potential of 162 mV. This result confirmed those previously obtained with respect to MUCS/Au and its union on the surface of the electrode, presented above. Line (b) represents the genosensor interaction with sNC/MUCS/Au (non-complementary DNA sequence). In this case, we obtained a current decrease of only 1.92% $I_{Relative}$. Such a poor current decrease indicated that the hybridization reaction of sNC (non-complementary sequence) with MUCS/Au was not taking place. Contrary, line (c) shows the hybridization of dsDNA/MUCS/Au with current decrease of the maximum anodic peak up to 10.52% of $I_{Relative}$ with respect to MUCS/Au, and 8.77% of $I_{Relative}$ in relation to sNC/MUCS/Au. This result was expected (see the above presented data) and established that the genosensor was able to discern between dsDNA-APC and sNC samples, which shows a strong selective capacity of our device.

Fig. 5B represents the cyclic voltammetry curves of $[Fe(CN)_6]^{3-/4-}$ obtained at SPGE previously modified with MUCS/Au (line a), while lines (b) and (c) shows the same process at SPGE modified with sNC/MUCS/Au and with dsDNA/MUCS/Au, after interaction with DOX. The line (b) in particular, shows the maximum anodic peak of DOX/sNC/MUCS/Au with current decrease of only 6.92% of $I_{Relative}$, respect to MUCS/Au. On the contrary, when DOX was added to dsDNA/MUCS/Au, the maximum anodic peak of DOX/dsDNA/MUCS/Au (line c) decreases for 16.82% of $I_{Relative}$ with respect to MUCS/Au.

These results confirmed that DOX was interspersed in the double-strand DNA sequences blocking the flow of $[Fe(CN)_6]^{3-/4-}$ ions as already mentioned above in the text. Definitively such effect is useful to increase the selectivity of our type of electrochemical DNA sensor. Therefore, it could be concluded that our genosensor is highly selective to detect target DNA *APC* gene. In a further step in the research, it would be possible to test other experimental conditions in order to improve the analyzing potential of this type of genosensors over the genetic material.

4. Conclusions

In summary, a systematic and detailed study was carried out following electrochemical bases to monitor the redox process of $[Fe(CN)_6]^{3-/4}$ on the SPGE electrode. This approach allowed us to develop a genosensor with the capacity to identify and measure the presence of an *APC* gene mutation through hybridization reactions under controlled conditions. In the study, SPGE was modified with MUCS, and the change was quantitatively concordant with a high degree of selectivity and sensitivity of our device. The genosensor allowed the detection of an *APC* mutation in a wide concentration range. The process was improved with the use of intercalating agents, which served as indicators of the hybridization reaction, particularly with DOX, a chemical that increased the sensitivity of the device operating at room temperature. In addition, the use of DOX did not alter the electrochemical response. Moreover, the results do not exclude the possibility of applying the detection of other genes using the same principle. The described genosensor seems to be a simple, accessible, and stable device, with rapid response and satisfactory reproducibility. Therefore, it would be an excellent option for preclinical studies related to carcinogenesis involving the *APC* gene, as well as to other DNA diagnoses or other biological biomarkers.

Acknowledgments

Luis Fernando Garcia-Melo thanks the CONACyT for the PhD scholarship (349230/237249) provided for Postgraduate studies (Ciencias Quimicobiológicas) in the Escuela Nacional de Ciencias Biológicas, Instituto Politécnico Nacional, Mexico City, Mexico.

We also thank CONACyT for financial support through the project INFR-2016-01-270227.

References

[1] M.J. Schell, M. Yang, J.K. Teer, F.Y. Lo, A. Madan, D. Coppola, A.N.A. Monteiro, M. V Nebozhyn, B. Yue, A. Loboda, G.A. Bien-Willner, D.M. Greenawalt, T.J. Yeatman, A multigene mutation classification of 468 colorectal cancers reveals a prognostic role for APC, Nat. Commun. 7 (2016) 11743. doi:https://doi.org/10.1038/ncomms11743.

[2] F. Yu, W. Cai, B. Jiang, L. Xu, S. Liu, S. Zhao, A novel mutation of adenomatous polyposis coli (APC) gene results in the formation of supernumerary teeth, J. Cell. Mol. Med. 22 (2018) 152–162, https://doi.org/10.1111/jcmm.13303.

[3] B.-Q. Li, P.-P. Liu, C.-H. Zhang, Correlation between the methylation of APC gene promoter and colon cancer, Oncol. Lett. 14 (2017) 2315–2319, https://doi.org/10.3892/ol.2017.6455.

[4] W. Hankey, W.L. Frankel, J. Groden, Functions of the APC tumor suppressor protein dependent and independent of canonical WNT signaling: implications for therapeutic targeting, Cancer Metastasis Rev. 37 (2018) 159–172, https://doi.org/10.1007/s10555-017-9725-6.

[5] E. Ayala-Calvillo, L.H. Mojica-Vázquez, A. García-Carrancá, L. González-Maya, Wnt/β-catenin pathway activation and silencing of the APC gene in HPV-positive human cervical cancer-derived cells, Mol. Med. Rep. 17 (2018) 200–208, https://doi.org/10.3892/mmr.2017.7853.

[6] X. Fu, J. Lin, F. Qin, Z. Yang, Y. Ding, Y. Zhang, L. Han, X. Zhu, Q. Zhang, LncAPC drives Wnt/β-catenin activation and liver TIC self-renewal through EZH2 mediated APC transcriptional inhibition, Mol. Carcinog. 57 (2018) 408–418, https://doi.org/10.1002/mc.22764.

[7] P.E. Kobayashi, C.E. Fonseca-Alves, L.G. Rivera-Calderón, M. Carvalho, H. Kuasne, S.R. Rogatto, R. Laufer-Amorim, Deregulation of E-cadherin, β-catenin, APC and Caveolin-1 expression occurs in canine prostate cancer and metastatic processes, Res. Vet. Sci. 118 (2018) 254–261, https://doi.org/10.1016/j.rvsc.2018.03.004.
[8] X. Qian, L. Ruan, APC gene promoter aberrant methylation in serum as a biomarker for breast cancer diagnosis: a meta-analysis, Thorac. Cancer 9 (2018) 284–290, https://doi.org/10.1111/1759-7714.12580.
[9] B. Wang, H. Song, H. Jiang, Y. Fu, X. Ding, C. Zhou, Early diagnostic potential of APC hypermethylation in esophageal cancer, Cancer Manag. Res. 10 (2018) 181–198, https://doi.org/10.2147/CMAR.S148677.
[10] N. Begam, K. Jamil, G.S. Raju, Promoter epigenetics of APC gene and its implication in sporadic breast cancer patients from South Indian population, Gene Reports, (2018), https://doi.org/10.1016/j.genrep.2018.04.004.
[11] L. Zhang, J.W. Shay, Multiple roles of APC and its therapeutic implications in colorectal cancer, JNCI J. Natl. Cancer Inst. 109 (2017) djw332-djw332. doi:https://doi.org/10.1093/jnci/djw332.
[12] V.S.P.K.S.A. Jayanthi, A.B. Das, U. Saxena, Recent advances in biosensor development for the detection of cancer biomarkers, Biosens. Bioelectron. 91 (2017) 15–23. doi:https://doi.org/10.1016/j.bios.2016.12.014.
[13] J. Wang, Electrochemical biosensors: towards point-of-care cancer diagnostics, Biosens. Bioelectron. 21 (2006) 1887–1892, https://doi.org/10.1016/j.bios.2005.10.027.
[14] K. Malecka, A. Stachyra, A. Góra-Sochacka, A. Sirko, W. Zagórski-Ostoja, H. Radecka, J. Radecki, Electrochemical genosensor based on disc and screen printed gold electrodes for detection of specific DNA and RNA sequences derived from Avian Influenza Virus H5N1, Sensors Actuators B Chem. 224 (2016) 290–297, https://doi.org/10.1016/j.snb.2015.10.044.
[15] S. Shahrokhian, R. Salimian, Ultrasensitive detection of cancer biomarkers using conducting polymer/electrochemically reduced graphene oxide-based biosensor: application toward BRCA1 sensing, Sensors Actuators B Chem. 266 (2018) 160–169, https://doi.org/10.1016/j.snb.2018.03.120.
[16] X. Wang, G. Shu, C. Gao, Y. Yang, Q. Xu, M. Tang, Electrochemical biosensor based on functional composite nanofibers for detection of K-ras gene via multiple signal amplification strategy, Anal. Biochem. 466 (2014) 51–58, https://doi.org/10.1016/j.ab.2014.08.023.
[17] N. Zhu, Z. Chang, P. He, Y. Fang, Electrochemical DNA biosensors based on platinum nanoparticles combined carbon nanotubes, Anal. Chim. Acta 545 (2005) 21–26, https://doi.org/10.1016/j.aca.2005.04.015.
[18] X. Fang, L. Bai, X. Han, J. Wang, A. Shi, Y. Zhang, Ultra-sensitive biosensor for K-ras gene detection using enzyme capped gold nanoparticles conjugates for signal amplification, Anal. Biochem. 460 (2014) 47–53, https://doi.org/10.1016/j.ab.2014.05.019.
[19] Z. Wang, Y. Yang, K. Leng, J. Li, F. Zheng, G. Shen, R. Yu, A sequence-selective electrochemical DNA biosensor based on HRP-labeled probe for colorectal cancer DNA detection, Anal. Lett. 41 (2008) 24–35, https://doi.org/10.1080/00032710701746873.
[20] F. Cecchet, M. Marcaccio, M. Margotti, F. Paolucci, S. Rapino, P. Rudolf, Redox mediation at 11-mercaptoundecanoic acid self-assembled monolayers on gold, J. Phys. Chem. B 110 (2006) 2241–2248, https://doi.org/10.1021/jp054290n.
[21] N.C. Tansil, H. Xie, F. Xie, Z. Gao, Direct detection of DNA with an electrocatalytic threading intercalator, Anal. Chem. 77 (2005) 126–134, https://doi.org/10.1021/ac0493469.
[22] C.-Y. Lee, P. Gong, G.M. Harbers, D.W. Grainger, D.G. Castner, L.J. Gamble, Surface coverage and structure of mixed DNA/Alkylthiol monolayers on gold: characterization by XPS, NEXAFS, and fluorescence intensity measurements, Anal. Chem. 78 (2006) 3326–3334, https://doi.org/10.1021/ac052137j.
[23] F. Kuralay, S. Campuzano, D.A. Haake, J. Wang, Highly sensitive disposable nucleic acid biosensors for direct bioelectronic detection in raw biological samples, Talanta. 85 (2011) 1330–1337, https://doi.org/10.1016/j.talanta.2011.06.012.
[24] F. Islam, M.H. Haque, S. Yadav, M.N. Islam, V. Gopalan, N.-T. Nguyen, A.K. Lam, M.J.A. Shiddiky, An electrochemical method for sensitive and rapid detection of FAM134B protein in colon cancer samples, Sci. Rep. 7 (2017) 133, https://doi.org/10.1038/s41598-017-00206-8.
[25] H. Fayazfar, A. Afshar, M. Dolati, A. Dolati, DNA impedance biosensor for detection of cancer, TP53 gene mutation, based on gold nanoparticles/aligned carbon nanotubes modified electrode, Anal. Chim. Acta 836 (2014) 34–44, https://doi.org/10.1016/j.aca.2014.05.029.
[26] T. Hianik, V. Gajdos, R. Krivanek, T. Oretskaya, V. Metelev, E. Volkov, P. Vadgama, Amperometric detection of DNA hybridization on a gold surface depends on the orientation of oligonucleotide chains, Bioelectrochemistry 53 (2001) 199–204, https://doi.org/10.1016/S0302-4598(00)00130-6.
[27] L. Tian, K. Qian, J. Qi, Q. Liu, C. Yao, W. Song, Y. Wang, Gold nanoparticles superlattices assembly for electrochemical biosensor detection of microRNA-21, Biosens. Bioelectron. 99 (2018) 564–570, https://doi.org/10.1016/j.bios.2017.08.035.
[28] S.R. Torati, V. Reddy, S.S. Yoon, C. Kim, Electrochemical biosensor for mycobacterium tuberculosis DNA detection based on gold nanotubes array electrode platform, Biosens. Bioelectron. 78 (2016) 483–488, https://doi.org/10.1016/j.bios.2015.11.098.
[29] K.Y.P.S. Avelino, I.A.M. Frias, N. Lucena-Silva, R.G. Gomes, C.P. de Melo, M.D.L. Oliveira, C.A.S. Andrade, Attomolar electrochemical detection of the BCR/ABL fusion gene based on an amplifying self-signal metal nanoparticle-conducting polymer hybrid composite, Colloids Surf. B: Biointerfaces 148 (2016) 576–584, https://doi.org/10.1016/J.COLSURFB.2016.09.029.
[30] F. Li, X. Han, S. Liu, Development of an electrochemical DNA biosensor with a high sensitivity of fM by dendritic gold nanostructure modified electrode, Biosens. Bioelectron. 26 (2011) 2619–2625, https://doi.org/10.1016/j.bios.2010.11.020.
[31] K. Hashimoto, K. Ito, Y. Ishimori, Novel DNA sensor for electrochemical gene detection, Anal. Chim. Acta 286 (1994) 219–224, https://doi.org/10.1016/0003-2670(94)80163-0.
[32] M. Kobayashi, T. Kusakawa, M. Saito, S. Kaji, M. Oomura, S. Iwabuchi, Y. Morita, Q. Hasan, E. Tamiya, Electrochemical DNA quantification based on aggregation induced by Hoechst 33258, Electrochem. Commun. 6 (2004) 337–343, https://doi.org/10.1016/j.elecom.2004.01.012.
[33] J.I.A. Rashid, N.A. Yusof, The strategies of DNA immobilization and hybridization detection mechanism in the construction of electrochemical DNA sensor: a review, Sens. Bio-Sens. Res. 16 (2017) 19–31, https://doi.org/10.1016/j.sbsr.2017.09.001.
[34] T. Tzyh-Chyang, H. Hsuan-Jung, Electrochemical studies of the intercalation of ethidium bromide to DNA, Electroanalysis 11 (1999) 1185–1190, https://doi.org/10.1002/(SICI)1521-4109(199911)11:16<1185::AID-ELAN1185>3.0.CO;2-#.
[35] M. Azimzadeh, N. Nasirizadeh, M. Rahaie, H. Naderi-Manesh, Early detection of Alzheimer's disease using a biosensor based on electrochemically-reduced graphene oxide and gold nanowires for the quantification of serum microRNA-137, RSC Adv. 7 (2017) 55709–55719, https://doi.org/10.1039/C7RA09767K.
[36] M. Yang, H.C.M. Yau, H.L. Chan, Adsorption kinetics and ligand-binding properties of thiol-modified double-stranded DNA on a gold surface, Langmuir. 14 (1998) 6121–6129, https://doi.org/10.1021/la980577i.
[37] L. Zhu, L. Luo, Z. Wang, DNA electrochemical biosensor based on thionine-graphene nanocomposite, Biosens. Bioelectron. 35 (2012) 507–511, https://doi.org/10.1016/j.bios.2012.03.026.
[38] G. Wang, J. Zhang, R.W. Murray, DNA binding of an ethidium intercalator attached to a monolayer-protected gold cluster, Anal. Chem. 74 (2002) 4320–4327, https://doi.org/10.1021/ac0257804.
[39] S.H. Minasyan, L.A. Tavadyan, A.P. Antonyan, H.G. Davtyan, M.A. Parsadanyan, P.O. Vardevanyan, Differential pulse voltammetric studies of ethidium bromide binding to DNA, Bioelectrochemistry. 68 (2006) 48–55, https://doi.org/10.1016/j.bioelechem.2005.03.006.
[40] A.C.H. de Castro, L.T. Kochi, A.C.R. Moço, R.S. Coimbra, G.C. Oliveira, S. Cuadros-Orellana, J.M. Madurro, A.G. Brito-Madurro, A new genosensor for meningococcal meningitis diagnosis using biological samples, J. Solid State Electrochem. 22 (2018) 2339–2346, https://doi.org/10.1007/s10008-018-3940-0.
[41] Y. Miao, Y. Li, Z. Zhang, G. Yan, Y. Bi, "Turn off–on" phosphorescent biosensors for detection of DNA based on quantum dots/acridine orange, Anal. Biochem. 475 (2015) 32–39, https://doi.org/10.1016/j.ab.2015.01.011.
[42] R.P.A. Balvedi, A.C.H. Castro, J.M. Madurro, A.G. Brito-Madurro, Detection of a specific biomarker for Epstein-Barr virus using a polymer-based genosensor, Int. J. Mol. Sci. 15 (2014) 9051–9066, https://doi.org/10.3390/ijms15059051.
[43] K. Kerman, D. Ozkan, P. Kara, B. Meric, J.J. Gooding, M. Ozsoz, Voltammetric determination of DNA hybridization using methylene blue and self-assembled alkanethiol monolayer on gold electrodes, Anal. Chim. Acta 462 (2002) 39–47, https://doi.org/10.1016/S0003-2670(02)00308-2.
[44] S. Wang, T. Peng, C.F. Yang, Investigation on the interaction of DNA and electroactive ligands using a rapid electrochemical method, J. Biochem. Biophys. Methods 55 (2003) 191–204, https://doi.org/10.1016/S0165-022X(02)00181-1.
[45] A. Banerjee, P. Majumder, S. Sanyal, J. Singh, K. Jana, C. Das, D. Dasgupta, The DNA intercalators ethidium bromide and propidium iodide also bind to core histones, FEBS Open Bio 4 (2014) 251–259, https://doi.org/10.1016/j.fob.2014.02.006.
[46] P. Kara, K. Kerman, D. Ozkan, B. Meric, A. Erdem, Z. Ozkan, M. Ozsoz, Electrochemical genosensor for the detection of interaction between methylene blue and DNA, Electrochem. Commun. 4 (2002) 705–709, https://doi.org/10.1016/S1388-2481(02)00428-9.
[47] C. Lin, Y. Wu, F. Luo, D. Chen, X. Chen, A label-free electrochemical DNA sensor using methylene blue as redox indicator based on an exonuclease III-aided target recycling strategy, Biosens. Bioelectron. 59 (2014) 365–369, https://doi.org/10.1016/j.bios.2014.03.053.
[48] F. Yao, J. Duan, Y. Wang, Y. Zhang, Y. Guo, H. Guo, X. Kang, Nanopore single-molecule analysis of DNA–doxorubicin interactions, Anal. Chem. 87 (2015) 338–342, https://doi.org/10.1021/ac503926g.
[49] H. Ilkhani, T. Hughes, J. Li, C.J. Zhong, M. Hepel, Nanostructured SERS-electrochemical biosensors for testing of anticancer drug interactions with DNA, Biosens. Bioelectron. 80 (2016) 257–264, https://doi.org/10.1016/j.bios.2016.01.068.
[50] C. Pérez-Arnaiz, N. Busto, J.M. Leal, B. García, New insights into the mechanism of the DNA/doxorubicin interaction, J. Phys. Chem. B 118 (2014) 1288–1295, https://doi.org/10.1021/jp411429g.
[51] H.C.M. Yau, H.L. Chan, M. Yang, Electrochemical properties of DNA-intercalating doxorubicin and methylene blue on n-hexadecyl mercaptan-doped 5′-thiol-labeled DNA-modified gold electrodes, Biosens. Bioelectron. 18 (2003) 873–879, https://doi.org/10.1016/S0956-5663(02)00161-6.
[52] T.H.M. Kjällman, H. Peng, C. Soeller, J. Travas-Sejdic, Effect of probe density and hybridization temperature on the response of an electrochemical hairpin-DNA sensor, Anal. Chem. 80 (2008) 9460–9466, https://doi.org/10.1021/ac801567d.
[53] C. Zhao, F. Gao, S. Weng, Q. Liu, L. Lin, X. Lin, An electrochemical sensor based on DNA polymerase and HRP-SiO2 nanoparticles for the ultrasensitive detection of K-ras gene point mutation, RSC Adv. 6 (2016) 8669–8676, https://doi.org/10.1039/C5RA24737C.
[54] N. Wu, W. Gao, X. He, Z. Chang, M. Xu, Direct electrochemical sensor for label-free DNA detection based on zero current potentiometry, Biosens. Bioelectron. 39 (2013) 210–214, https://doi.org/10.1016/j.bios.2012.07.038.
[55] V.G.S. Box, The intercalation of DNA double helices with doxorubicin and nagalomycin, J. Mol. Graph. Model. 26 (2007) 14–19, https://doi.org/10.1016/j.jmgm.2006.09.005.

[56] X. Chu, G.-L. Shen, J.-H. Jiang, T.-F. Kang, B. Xiong, R.-Q. Yu, Voltammetric studies of the interaction of daunomycin anticancer drug with DNA and analytical applications, Anal. Chim. Acta 373 (1998) 29–38, https://doi.org/10.1016/S0003-2670(98)00362-6.

[57] D. Agudelo, P. Bourassa, G. Bérubé, H.-A. Tajmir-Riahi, Intercalation of antitumor drug doxorubicin and its analogue by DNA duplex: structural features and biological implications, Int. J. Biol. Macromol. 66 (2014) 144–150, https://doi.org/10.1016/j.ijbiomac.2014.02.028.

[58] C.-P. Hsu, Y.-F. Huang, Y.-L. Wang, Investigation of the non-faradaic current of DNA-immobilized microelectrodes in concentrated salt environment for biosensors, ECS J. Solid State Sci. Technol. 5 (2016) Q149–Q154, https://doi.org/10.1149/2.0141606jss.

[59] E.F. Silva, R.F. Bazoni, E.B. Ramos, M.S. Rocha, DNA-doxorubicin interaction: new insights and peculiarities, Biopolymers 107 (2017) e22998, , https://doi.org/10.1002/bip.22998.

[60] M. Taei, F. Hasanpour, H. Salavati, S. Mohammadian, Fast and sensitive determination of doxorubicin using multi-walled carbon nanotubes as a sensor and CoFe2O4 magnetic nanoparticles as a mediator, Microchim. Acta 183 (2016) 49–56, https://doi.org/10.1007/s00604-015-1588-3.

[61] J. Vacek, L. Havran, M. Fojta, Ex situ voltammetry and chronopotentiometry of doxorubicin at a pyrolytic graphite electrode: redox and catalytic properties and analytical applications, Electroanalysis 21 (2009) 2139–2144, https://doi.org/10.1002/elan.200904646.